Phys. Chem. Glasses: Eur. J. Glass Sci. Technol. B, August 2011, **52** (4), 157–166

Free volume and energy barriers to equilibrium viscosity and ionic transport in alkali disilicates

Marcio Luis Ferreira Nascimento,[1] *Ana Candida Martins Rodrigues*[2]* *& Jean-Louis Souquet*[3]

[1] *Instituto de Humanidades, Artes & Ciências, Universidade Federal da Bahia, Rua Barão de Jeremoabo s/n, PAF 3, Campus Universitário de Ondina, 40170-115 Salvador-BA, Brasil*
[2] *Laboratório de Materiais Vítreos, Departamento de Engenharia de Materiais, Universidade Federal de São Carlos, 13565-905 São Carlos-SP, Brasil*
[3] *Permanent address: Laboratoire d'Electrochimie et de Physicochimie des Matériaux et des Interfaces, PHELMA, BP 75, 38402 Saint Martin D'Hères Cedex, France*

Manuscript received 21 January 2011
Revised version received 5 April 2011
Accepted 9 April 2011

A microscopic interpretation is developed of the temperature dependence of viscosity above the glass transition range, validating the representation of experimental data by a "hybrid" equation, which is a product of Arrhenius and Vogel–Fulcher–Tamman–Hesse (VFTH) exponential terms. By employing this hybrid equation to fit experimental viscosity data for lithium, sodium, and potassium disilicates, we found an activation energy of $E_\eta^A \approx 1{\cdot}2$ *eV for the Arrhenius term. We propose that this energy is representative of the exchange of nonbridging oxygen atoms between adjacent* SiO_4 *tetrahedra, allowing for consecutive relaxations of macromolecular silicate chains. Based on a free volume interpretation of the VFTH term, we also calculated the free volume required for chain movement, which, according to our results, is about 30% of the intrinsic volume of chain segments. This relatively low free volume may indicate the occurrence of limited rotational or translational displacements during viscous flow. These results are discussed and compared with the activation enthalpies and free volumes determined for ionic transport in the same alkali disilicate glasses considering a similar "hybrid" equation for electrical conductivity.*

1. Introduction

The viscosity of a fluid expresses the facility of its constitutive species, i.e. atoms, molecules or macromolecules, to move in the surroundings of their neighboring species. From this standpoint, viscosity clearly depends on the fluid's interatomic or intermolecular interactions and atomic density.

From a macroscopic standpoint, viscosity, η, is defined as the proportionality coefficient between a shearing stress σ_{xy} and the rate of deformation $\delta\varepsilon_{xy}/\delta t$ when a linear relationship links these two measurable quantities, i.e.

$$\sigma_{xy} = \eta \frac{\dot{\varepsilon}_{xy}}{\dot{t}} \quad (1)$$

leading η to be measured in Pa s. Viscosity may vary over 26 orders of magnitude from 2×10^{-2} Pa s (for air at room temperature) to an estimated value of 10^{24} Pa s in the continental mantle, at higher temperatures and pressures. At values exceeding 10^{13} Pa s, the strain rate is hardly measurable on a human time scale and the material is considered to be a solid. Therefore, most of available viscosity data for oxide glasses are for viscosities below 10^{13} Pa s.

In glass technology, viscosity determines melting conditions, raw material dissolution rates, removal of bubbles, working and annealing temperatures, and crystallization rates. The practical variation of viscosity with temperature of usual glass forming melts currently covers 13 orders of magnitude, from 10^1 to 10^{13} Pa s. Due to the technological importance of viscosity, many empirical and useful expressions have been proposed to predict viscosity dependence on temperature or composition,[1,2] but in many cases, the correspondence with experimental data introduces interdependent fitting parameters whose physical meaning is not always clearly established.

This work focuses on a microscopic approach to viscosity. This approach allows some of the available parameters commonly involved in the expressions describing viscosity temperature dependence to be determined numerically, and thus, the total number of adjustable parameters to be minimized, enabling a more accurate physical interpretation of the remaining ones. We have applied this approach to three alkali disilicates for which numerous viscosity data are available.[3]

The energy and steric barriers deduced from this approach are discussed considering similar barriers inferred in a previous study[4] on ionic transport, which were calculated using a similar approach and for the same compositions and temperature range as those investigated here for viscosity data.

* Corresponding author. Email acmr@ufscar.br

2. Temperature dependence of experimental viscosity data

Viscosity is currently determined in a wide range of 10^1 to 10^{13} Pa s. In a first approximation, the temperature dependence of experimental viscosity data above the glass transition temperature, T_g, follows the empirical Vogel–Fulcher–Tammann–Hesse (VFTH) equation

$$\eta = \eta_0 \exp\left(\frac{C_\eta}{T - T_0}\right) \tag{2}$$

where η_0, C_η and T_0 are constants in a given temperature range and depend on the composition of the glass forming melt. In this expression, C_η and T_0 have dimensions of Kelvin.

This relationship, designated here as the VFTH equation, was proposed independently between 1920 and 1926 by Vogel[5] for the temperature dependence of the viscosity of greases, by Fulcher[6] for silicate glasses, and by Tammann & Hesse[7] for glass forming organic liquids.

If C_η is substituted by B_η/k_B where k_B is the Boltzmann constant, the VFTH equation can be expressed as

$$\eta = \eta_0 \exp\left[\frac{B_\eta}{k_B (T - T_0)}\right] \tag{3}$$

where B_η has units of energy.

Whether Equation (2) or (3) is chosen, the empirical VFTH equation is justified by either the "free volume theory" developed by Cohen & Turnbull[8] or the "entropic model" of Adams & Gibbs,[9] as will be discussed later herein.

An improvement of the VFTH equation was proposed by Dienes[10] and later by Macedo & Litovitz[11] through the addition of an enthalpic term, E_η^A. This new equation, which we will call the DML equation, can be expressed as

$$\eta = \eta_0 \exp\left(\frac{E_\eta^A}{k_B T}\right) \exp\left[\frac{B_\eta}{k_B (T - T_0)}\right] \tag{4}$$

This expression is also called a "hybrid equation" because it combines an Arrhenius exponent with a VFTH one. It has been found that the DML equation conveniently represents the temperature dependence of the viscosity of liquids with very different molecular or atomic cohesive forces, from van der Waals and hydrogen bonds to metallic and covalent bonds, including polymers.[10,11]

Fitting experimental data with the VFTH Equation (3) leads to the assessment of three parameters: η_0, B_η and T_0. However, when experimental viscosity data are fitted to the DML Equation (4), a fourth parameter, E_η^A, can also be determined. Obviously, Equations (3) and (4) do not lead to the same numerical values for the three common parameters. Furthermore, they depend on the microscopic interpretation of the viscosity mechanism.

3. Microscopic aspects of viscosity

3.1 Basic formalism

From a microscopic standpoint, viscosity, η, is related to the relative displacement of a liquid's constitutive molecules or, in the case of a macromolecular network like a molten silicate, to the ability of chain segments to move in the supercooled liquid phase. These elementary displacements are characterized by a structural relaxation time, τ_η, which is the average time for a molecule or chain segment to move a distance λ_η comparable to its size. The dependence of viscosity on these microscopic parameters can be determined by identifying two different expressions for the diffusion coefficient, D_η, of the moving specie(s), as detailed below.

The first expression derives from the generalized Einstein relation, in which D_η is proportional to the temperature T, and the mobility μ of the moving species

$$D_\eta = \mu k_B T \tag{5}$$

The mobility μ is defined as the ratio of the particle's terminal drift velocity v_d to an applied force F, i.e.

$$\mu = \frac{v_d}{F} \tag{6}$$

The mobility μ can also be written as a function of λ_η and η[12]

$$\mu = \frac{1}{\lambda_\eta \eta} \tag{7}$$

thus leading to

$$D_\eta = \frac{k_B T}{\lambda_\eta \eta} \tag{8}$$

Equation (8) is similar, apart from a factor of 3π, to the Stokes–Einstein law which makes the additional hypothesis of a spherical shape for the different diffusing species. This relation is always valid as long as diffusion and viscosity are controlled by the same atomic species and the same mechanism.

Another expression for D_η derives from the Brownian motion

$$D_\eta = \frac{\lambda_\eta^2}{\tau_\eta} \tag{9}$$

and combining Equations (8) and (9) gives

$$\eta = \frac{k_B T \tau_\eta}{\lambda_\eta^3} \tag{10}$$

The structural relaxation time, τ_η, can, in turn, be expressed as the reciprocal product of the attempt frequency ν_0 of the moving species by the probability Ω of a successful jump

$$\tau_\eta = \frac{1}{\nu_0 \Omega} \tag{11}$$

Finally, the viscosity η can be written as

$$\eta = \frac{k_B T}{\lambda_\eta^3 \nu_0 \Omega} \tag{12}$$

Therefore, this equation links time and the elementary atomic displacements to the viscosity. Several microscopic models have been proposed to validate the behaviour of viscosity in response to temperature and are discussed below. These models differ from each other only by their different approaches to describing the jump probability, leading to different expressions for Ω, all of which are exponential functions of temperature.

3.2 Free volume theory

The "free volume theory" developed by Cohen & Turnbull[5] to justify the VFTH equation supposes that a molecule, or a chain segment, rattles in the cage formed by its nearest neighbours until the random density fluctuations produce an adjoining cage large enough to enable a jump from one cage to another. These fluctuations involve the exchange of a so-called "free" volume between the two neighbouring cages. The term "free" means that this volume transfer occurs without any enthalpic cost, since the enthalpy to increase the size of a cage is compensated locally by the enthalpy released from the contraction of the initial adjacent cage. In this case, the displacement probability is an exponential function of the ratio between the smallest or critical free volume V_η^{f*} necessary for a jump and the mean free volume, $\bar{V}_\eta^{f}$, available to the moving species

$$\Omega = \exp\left(-\frac{V_\eta^{f*}}{\bar{V}_\eta^{f}}\right) \tag{13}$$

The available mean free volume is usually approximated by a linear function of T

$$V_\eta^{f} \approx V_{0\eta}(\alpha_l - \alpha_c)(T - T_0) \tag{14}$$

where α_l and α_c are the thermal expansion coefficients of the liquid and corresponding crystal and $V_{0\eta}$ is the volume occupied by the moving species in the crystal at T_0.

Equation (14) assumes that the free volume essentially consists of the difference between the total liquid expansion ($\alpha_l V_{0\eta}$) and the vibrational expansion ($\alpha_c V_0$). Note that α_c can be replaced by the thermal expansion coefficient of the glass, α_g, since the amplitudes of the atomic vibrations are comparable in the crystalline and glassy states, i.e. $\alpha_c \approx \alpha_g$.

Finally, substituting Equations (13) and (14) in Equations (11) and (12), shows that the structural relaxation time τ_η and viscosity η can be expressed, respectively, by

$$\tau_\eta = \frac{1}{\nu_0}\exp\left[\frac{V_\eta^{f*}}{V_{0\eta}(\alpha_l - \alpha_c)(T - T_0)}\right] \tag{15}$$

and

$$\eta = \frac{k_B T}{\lambda_\eta^3 \nu_0}\exp\left[\frac{V_\eta^{f*}}{V_{0\eta}(\alpha_l - \alpha_c)(T - T_0)}\right] \tag{16}$$

Equation (16) corresponds to the VFTH Equation (3) with

$$\frac{B_\eta}{k_B} = \frac{V_\eta^{f*}}{V_{0\eta}(\alpha_l - \alpha_c)} \tag{17}$$

in which T_0 is no longer an empirical parameter but the extrapolated temperature at which the specific volume of the liquid would be the same as that of the crystal. Thus on cooling as $T \to T_0$, τ_η and η tend towards infinity. T_0, which can be determined by the extrapolation of these kinetic quantities, is called the ideal glass transition temperature. Using Equation (16) to fit viscosity data, $V_\eta^{f*}/V_{0\eta}$ ratios have been estimated for van der Waals liquids, liquid metals[8] and borates and silicates melts.[13]

3.3 Adam–Gibbs theory

A different approach to molecular rearrangements above T_g, which was developed by Adam & Gibbs,[9] suggests that the supercooled liquid relaxes by cooperative, i.e. interdependent movements of several molecules or chain segments. The probability of a cooperative displacement involving a number z of neighbouring species can be written as

$$\Omega = \exp\left(-\frac{z\Delta\mu}{k_B T}\right) \tag{18}$$

where $\Delta\mu$ is the free energy necessary for each elementary displacement. This number z is given by the ratio of the entropy s_c^* associated with an elementary displacement to the available configurational molar entropy S_c in the supercooled liquid, i.e.

$$\frac{z}{N_A} = \frac{s_c^*}{S_c} \tag{19}$$

where N_A is Avogadro's number. According to Kauzmann,[14] this configurational entropy decreases with temperature and disappears at a temperature T_K at which the entropy of the supercooled liquid would be the same as that of the crystal of the same composition. Since s_c^* is a constant characteristic of an elementary displacement, when $T \to T_K$, z increases and Ω tends to zero, while the viscosity tends to infinity. According to this model, viscosity can be expressed as

$$\eta = \frac{k_B T}{\lambda_\eta^3 \nu_0}\exp\left[\frac{s_c^* N_A \Delta\mu}{k_B T S_c}\right] \tag{20}$$

or assuming that all the microscopic characteristics are constants

$$\eta = \eta_{0(T)}\exp\frac{C}{TS_c} \tag{21}$$

The configurational entropy of the supercooled liquid is expressed as

$$S_c = \int_T^{T_k} \frac{\Delta C_p}{T} \mathrm{d}T \tag{22}$$

where ΔC_p is the difference between the heat capacity of the liquid and the crystal. When ΔC_p data are available as a function of T, S_c can be calculated as a function of temperature, and a linear variation of $\log \eta$ as a function of $1/(TS_c)$ is effectively observed,[15] as expected from Equation (21).

When calorimetric data are not available, ΔC_p can be approximated[16] by

$$\Delta C_p \approx \frac{D}{T} \tag{23}$$

(with D constant); thus, S_c can be written as

$$S_c \approx \frac{D(T - T_K)}{TT_K} \tag{24}$$

This approach finally leads to an expression for the viscosity temperature dependence which is formally comparable to Equations (3) and (16), but with different interpretations for the parameters B_η and T_0, namely

$$\eta = \frac{k_B T}{\lambda_0^3 \nu_0} \exp \frac{B_\eta}{k_B (T - T_K)} \tag{25}$$

where

$$B_\eta = \frac{s_c^* N_A \Delta\mu T_K}{D} \tag{26}$$

It has been shown that for most glass forming liquids for which kinetic *and* thermodynamic data are available, the extrapolated values of T_0 (kinetic) as defined by Cohen & Turnbull,[8] and the Kauzmann temperature, T_K (thermodynamic), are often similar,[17] however there are some notable exceptions, e.g. for strong glasses.[18] At T_K or T_0, cooperative atomic displacements that control viscous flow are supposed to cease, and consequently, viscosity diverges to infinity.

The divergence of viscosity due to the vanishing of configurational entropy at the Kauzmann temperature has been questioned recently by Mauro *et al*.[19] To avoid such a possibility, the hypothesis that the configurational entropy completely vanishes at T_K was replaced by a reasonably expected slow decrease down to 0 K.[19] However, all these considerations concern non-equilibrium viscosity below T_g. Furthermore, in the absence of experimental data, Equation (25) cannot be tested in a wide temperature range below T_g, and it therefore remains a good approximation to describe the temperature dependence of the equilibrium viscosity (above T_g).

3.4 The Dienes–Macedo–Litovitz model

The DML equation, applied as an improvement over the free volume model, suggests that the jump probability Ω is the product of two independent probabilities, Ω_1 and Ω_2

$$\Omega = \Omega_1 \times \Omega_2 = \exp\left(-\frac{E_\eta^A}{k_B T}\right) \exp\left(-\frac{V_\eta^{f*}}{\overline{V}_f}\right) \tag{27}$$

This equation introduces an enthalpic parameter, E_η^A, in an Arrhenius exponent, independent of the free volume term. According to Macedo & Litovitz,[11] this enthalpic parameter represents the activation energy necessary to separate the individual diffusing units from their neighbours. The second exponential is related to the transfer of these units by a free volume mechanism from one site to a neighbouring one. Thus, more than merely a mathematical improvement, this expression formally dissociates a temperature-activated event from the rearrangements of the surrounding liquid phase represented by the second exponent. Both the activated event and molecular rearrangements contribute to the glass relaxation.

Combining Equation (27) for the jump probability with Equation (14) for the mean available free volume and Equation (12) for viscosity, one obtains the following relation for the temperature dependence of viscosity

$$\eta = \frac{k_B T}{\lambda_\eta^3 \nu_0} \exp\left(\frac{E_\eta^A}{k_B T}\right) \exp\left[\frac{B_\eta}{k_B (T - T_0)}\right] \tag{28}$$

Depending on the relative importance of the two exponentials, the viscosity of a supercooled liquid may present an Arrhenius behaviour, as found in silica, or tend to a pure VFTH one.

In their original paper, Macedo & Litovitz[11] used the free volume model to justify the temperature dependence of the second exponent. Nevertheless, an identical expression could be derived using the Adam–Gibbs[9] model, replacing the ideal glass transition temperature, T_0, with the Kauzmann temperature, T_K. In both approaches, E_η^A represents an activation energy closely associated to the relaxation of the neighbouring molecules or chain segments.

3.5 Assessment of the pre-exponential term

We also point out that the pre-exponential term in Equation (28) is temperature-dependent. To eliminate this dependence, this expression can also be written as

$$\frac{\eta}{T} = A_\eta \exp\left(\frac{E_\eta^A}{k_B T}\right) \exp\left[\frac{B_\eta}{k_B (T - T_0)}\right] \tag{29}$$

where

$$A_\eta = \frac{k_B}{\lambda_\eta^3 \nu_0} \tag{30}$$

is a temperature independent pre-exponential term, which can be estimated numerically. In fact, taking λ_η=5 Å, ν_0=10^{13} Hz, results in A_η=10^{-8} Pa s/K.

In the classical VFTH expression

$$\eta_0 = A_\eta T \tag{31}$$

and is therefore temperature-dependent. However, in the temperature range in which experimental viscosity data are usually collected, the variation of Equation (31) is much lower than the variation of the exponential term of Equation (3). Thus, assuming a mean value of 1000 K for the temperature T at which viscosity is measured, the pre-exponential term can be estimated to be $\eta_0=10^{-5}$ Pa s. This value has been shown to give the best fit using a single VFTH equation for oxide melts with fixed η_0.[20,21] Considerations related to the concept of strong and fragile supercooled liquids also lead to this η_0 value.[22] However, it is worth noting that when experimental data are fitted using the VFTH equation with three adjustable parameters (η_0, B_η, and T_0), a great variation of η_0 values is found, ranging from 1 to 10^{-5} Pa s.[2,23,24]

Another estimation of η_0 can be assessed using the Maxwell relation between the viscosity, η, the shear modulus at infinite frequency, G_∞, and the structural relaxation time, τ_η, i.e.

$$\eta = G_\infty \tau_\eta \tag{32}$$

At high temperature, τ_η should tend to 10^{-13} s and since G_∞, which is associated with bond stiffness, is generally estimated between 1 and 10 GPa, η_0 should be close to 10^{-4} to 10^{-3} Pa s.

Whatever the extrapolated value of η_0 may be, this pre-exponential term is formally temperature-dependent and justifies the choice of η/T coordinates rather than η when viscosity is plotted as a function of temperature. We will use Equation (29) to fit experimental data on lithium, sodium and potassium disilicates. We will then propose a possible interpretation of the parameters E_η^A and B_η at a microscopic level.

4. Analysis of alkali disilicate viscosity data

4.1 Determination of the DML equation parameters

We collected experimental data from different authors[25–59] on the alkali disilicates $Li_2O.2SiO_2$,[25–36] $Na_2O.2SiO_2$[25,30,34,37–58] and $K_2O.2SiO_2$[25,31,32,57] over the temperature range of 650 to 1800 K, covering twelve orders of magnitude of viscosity, from 10 to 10^{13} Pa s. These data are reported in Figures 1(a), (b) and (c), using $\log(\eta/T)=f(T)$ coordinates, and were fitted with DML Equation (29), which contains *a priori* four adjustable parameters, A_η, B_η, T_0 and E_η^A. Generally, when fitting experimental data with four adjustable parameters, it is always possible to obtain a good fit. This is especially valid in the case of Equation (29), which contains the product of two temperature-dependent exponents, and successive fits may lead to different sets of the floating parameters. We then restricted the number of adjustable parameters by fixing the ideal glass transition temperature T_0 and the pre-exponential term A_η at realistic values, as detailed below. The two remaining parameters, B_η, and E_η^A, for which we will propose a microscopic interpretation, were then determined by fitting.

The ideal glass transition temperature, T_0, is estimated from the experimental glass transition, T_g. In fact, using two semi-empirical laws which relate T_0 and T_g to the melting temperature, T_m, of the crystalline phase, i.e. $T_g \approx (2/3)T_m$ and $T_0 \approx (1/2)T_m$, leads to $T_0 \approx (3/4)T_g$.[1] For lithium, sodium and potassium disilicates, we then estimated T_0=545 K, 551 K and 568 K, respectively. Following section 3.5, A_η was fixed at a value of 10^{-8} Pa s/K.

All adjustments were performed using Levenberg–Marquardt nonlinear fitting and the Origin™ software package. Table 1 gives the number N of collected experimental viscosity data and the respective χ^2 results for each composition. The data are more numerous for sodium disilicate, which leads to the worst χ^2 results. However, from a statistical standpoint, the resulting viscosity fit is more reliable because it corresponds to an average value from different sources, authors, experimental procedures and possible slight compositional differences. The resulting values for the B_η and E_η^A parameters are also reported in Table 1. Calculated curves using the DML parameters are shown as full lines in Figures 1(a) to (c).

Note that with E_η^A=0, Equation (29) reduces to a VFTH type equation

$$\frac{\eta}{T} = A_\eta \exp\left[\frac{B_\eta}{k_B (T - T_0)}\right] \tag{33}$$

which cannot be fitted to experimental data when A_η and T_0 are fixed at the values reported in Table 1. A good fit can be obtained only with very different and physically unrealistic A_η and T_0 parameters.

4.2 Microscopic interpretation of viscosity parameters from the hybrid DML equation

4.2.1 The Arrhenius term

We suggest here that the activation energy E_η^A of the Arrhenius exponent in the DML Equation (29) may be associated with the molecular rearrangements that induce relaxation of the surrounding liquid phase, which, in turn, is described by the VFTH exponent. Numerical values of E_η^A found for the three disilicates and listed in Table 1 are close to 1·2 eV. This value is independent of the nature of the alkali cation, which suggests that this energy is not associated with chemical bonds involving the alkali cation. Thus, this energy may be related to a reorganization of the silicon–oxygen tetrahedra involving nonbridging oxygens. A model for this atomic rearrangement was proposed by Farnan & Stebbins,[60] which describes the switching of bridging oxygen and nonbridging oxygen involving two SiO_4 tetrahedra. In fact, the rate

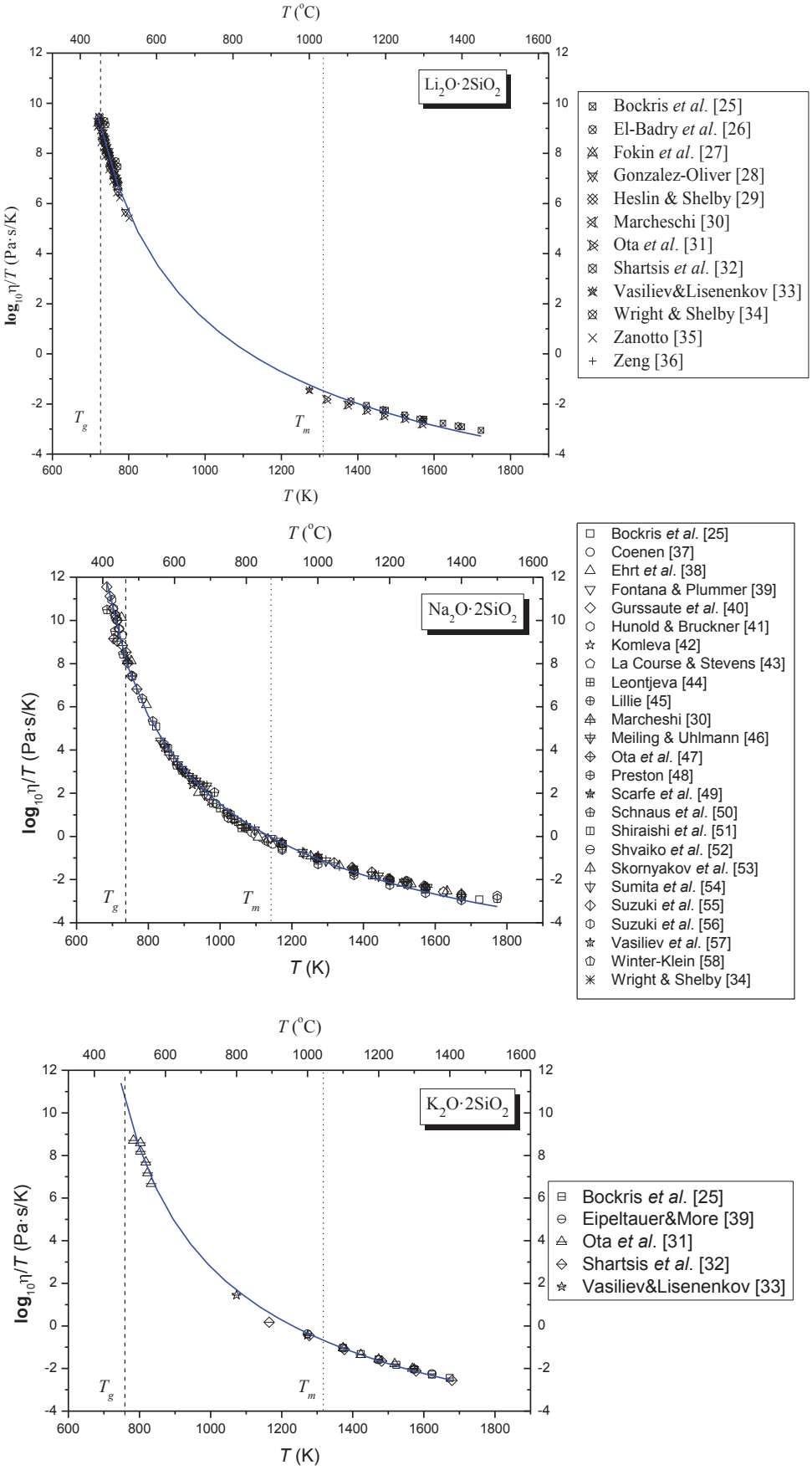

Figure 1. Experimental viscosity data[25–59] on binary lithium (a), sodium (b) and potassium (c) disilicate glass (symbols) fitted by the Dienes–Macedo–Litovitz Equation (29) (full line) using the parameters listed in Table 1. The dotted lines indicate the corresponding glass transition temperatures, T_g*, and the disilicate melting temperatures,* T_m

Table 1. Numerical values for E_η^A *(eV) and* B_η *(eV) obtained by the best fit of experimental data using the DML Equation (29). The pre-exponential terms* A_η *and* T_0 *were fixed at* 10^{-8} *Pas/K and 0·75*T_g*, respectively. The corresponding number* N *of experimental data and* χ^2 *values are also reported. The mathematical accuracy is of* $\pm 2\times10^{-2}$ *eV and* $\pm 5\times10^{-3}$ *eV for* E_η^A *and* B_η*, respectively*

Melt composition	A_η *(Pas/K)*	T_g *(K)*	T_0 *(K)*	E_η^A *(eV)*	B_η *(eV)*	N	χ^2
$Li_2O.2SiO_2$	10^{-8}	727	545	1·13	0·329	76	0·030
$Na_2O.2SiO_2$	10^{-8}	735	551	1·27	0·274	137	0·055
$K_2O.2SiO_2$	10^{-8}	757	568	1·20	0·404	31	0·021

of coordination change between two different silicon surroundings ($Q^3 \Rightarrow Q^4$) was determined using ^{29}Si NMR in the K_2O–$4SiO_2$ composition and effectively found to be closely related on a time scale to the relaxation time measured from viscosity data.[60]

However, pure silica shows a different behaviour, since its macromolecular network has a higher covalent character than that of alkali silicate. In this case, the DML equation reduces to the Arrhenius exponent with much higher corresponding activation energy, E_η^A of 6·1 eV,[61] than that found for alkali disilicates. The significant difference between the activation energies of silica and alkali silicates is consistent with the idea that, in the case of alkali disilicates, the presence of nonbridging oxygens reduces the energy required to initiate a local atomic reorganization.

4.2.2 The VFTH term

The second exponent, or the VFTH term of Equation (29), can be discussed in terms of the free volume model proposed by Cohen & Turnbull or the entropic model proposed by Adam & Gibbs. However, as mentioned earlier, in the entropic model, it was found that B_η was given by Equation (26). In this equation, s_c^* and $\Delta\mu$ are not easily dissociable, making any quantitative interpretation of B_η too speculative. Thus, only the free volume model will be used to interpret results concerning B_η.

According to the free volume model, the B_η parameter in Table 1 depends on the ratio of the critical free volume V_η^{f*} associated with the displacement of an entity whose volume would be $V_{0\eta}$ at the temperature T_0 at which the free volume disappears. The $V_\eta^{f*}/V_{0\eta}$ ratio can be calculated using Equation (17), where α_l and α_g represent the volumetric thermal expansion of the liquid and corresponding glass. Table 2 lists the α_l and α_g values found for the three alkali disilicates under study and their calculated $V_\eta^{f*}/V_{0\eta}$ ratios.

In Table 2, the $V_\eta^{f*}/V_{0\eta}$ ratios are close to 0·3 for the three compositions, indicating that the displacement of silicate chains requires a three-fold lower free volume than that occupied by the chain segment itself at T_0. This low $V_\eta^{f*}/V_{0\eta}$ ratio suggests that the viscous flow of alkali disilicates is governed by limited or low amplitude rotational or translational movements. Figure 2 depicts a possible oxygen atom switching mechanism correlated with local reorganization of the neighbouring SiO_4 tetrahedra.

Table 2. Volumetric thermal expansion coefficients in the liquid (α_l) *and glassy* (α_g) *states and calculated volume ratios* $V_\eta^{f*}/V_{0\eta}$.[62,63] *(a) For potassium disilicate,* α_l *was calculated from density data*[2]

Melt composition	α_l $(\times10^{-7}/K)$	α_g $(\times10^{-7}/K)$	$V_\eta^{f*}/V_{0\eta}$
$Li_2O.2SiO_2$	1119*	361*	0·29
$Na_2O.2SiO_2$	1395**	495**	0·29
$K_2O.2SiO_2$	1455[a]	558**	0·42

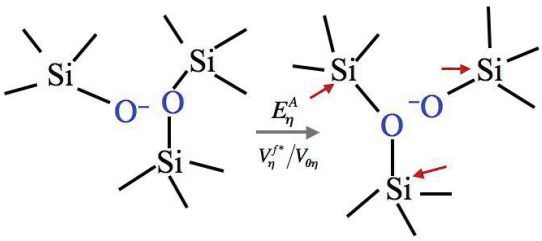

Figure 2. Schematic representation of a nonbridging oxygen (NBO) and bridging oxygen (BO) switching mechanism associated with a local reorganization of the neighbouring SiO_4 *tetrahedra. The red arrows indicate the atomic displacement from the initial position*

4.3 Comparison with ionic transport above T_g

Previously[4] we employed the DML equation

$$\sigma T = A\exp\left(-\frac{E_\sigma^A}{k_B T}\right)\exp\left[-\frac{B_\sigma}{k_B\left(T-T_0\right)}\right] \qquad (34)$$

to interpret the dependence of ionic conductivity (σ) on temperature above T_g of lithium, sodium and potassium disilicates. In this expression, E_σ^A represents the energy required for the formation of the charge carrier, and B_σ is related to its migration in the macromolecular network.

Based on an interpretation similar to that developed here for viscosity, B_σ is also related to a free volume ratio $V_\sigma^{f*}/V_{0\sigma}$ by

$$V_\sigma^{f*}/V_{0\sigma} = B_\sigma(\alpha_l - \alpha_g)/k_B \qquad (35)$$

Using a similar mathematical procedure as the one described above for viscosity data, E_σ^A and $V_\sigma^{f*}/V_{0\sigma}$ were also determined using Equation (34) to fit experimental data. The resulting values of E_η^A and $V_\sigma^{f*}/V_{0\sigma}$, are listed in Table 3, together with the corresponding viscosity parameters for purposes of comparison. As can be seen from Table 3, the activation energy for ionic transport, E_σ^A, is close to 0·5 eV and the V_σ^{f*}/V_0 ratio is about 3×10^{-2}.

As mentioned earlier, the proposed microscopic model for ionic transport[4] assumes that the activa-

Table 3. Viscous flow and ionic transport activation energies E_η^A *and* E_σ^A *and corresponding free volume ratios* $V_\eta^{f*}/V_{0\eta}$ *and* $V_\sigma^{f*}/V_{0\sigma}$. E_s^A *and* $V_\sigma^{f*}/V_{0\sigma}$ *are taken from Ref. 4*

Melt composition	E_η^A *(eV)*	E_η^A *(eV)*	$V_\eta^{f*}/V_{0\eta}$	$V_\sigma^{f*}/V_{0\sigma}$
$Li_2O.2SiO_2$	1·13	0·48	0·29	0·037
$Na_2O.2SiO_2$	1·27	0·51	0·29	0·034
$K_2O.2SiO_2$	1·20	0·55	0·42	0·039

tion energy E_σ^A represents the energy required to create a charge carrier and $V_\sigma^{f*}/V_{0\sigma}$ represents the free volume ratio required for its migration in the electric field.

From a microscopic standpoint, it has been proposed that alkali transport occurs through an interstitial cationic pair composed of two alkali cations sharing the same negatively charged nonbridging oxygen.[64–66] The formation of an interstitial cationic pair thus results from the dissociation of an alkali cation bound ionically to a nonbridging oxygen, allowing it to jump to a neighbouring cationic site that is already occupied.[4] This site, occupied by two alkali cations, is positively charged and the excess cation may be transferred from one nonbridging oxygen to another, enabling the displacement of the positive charge along the macromolecular silicate chains. The formation of a cationic pair implies the reorganization of ionic bonds, and a lower activation energy is expected than that required for the reorganization of the Si–O covalent bonds in the viscous flow, thus qualitatively justifying $E_\sigma^A<E_\eta^A$.

The free volume ratio related to conductivity, $V_\sigma^{f*}/V_{0\sigma}$, represents the ratio of the critical free volume required for the transfer of an interstitial cationic pair from one nonbridging oxygen to another at a temperature above T_g. This ratio is one order of magnitude lower than the equivalent viscosity ratio ($V_\eta^{f*}/V_{0\eta}$). This lower ratio is consistent with the idea that viscous flows imply chain segment displacements, whereas ionic transport above T_g is assisted only by more localized movements of chain segments. These localized movements of low amplitude could be attributed tentatively to vibrations of nonbridging oxygen atoms which allow for the transfer of an alkali cation from one bridging oxygen to another. This transfer mechanism implies an exchange in the coordination number between two neighbouring nonbridging oxygens, and from this standpoint, it can be compared to the transfer of protons in water by the so-called "Grotthus mechanism".[67]

Another approach to relate ionic transport and viscosity can be assessed by means of the correlation of the diffusion coefficient D_η as expressed by Equation (8) with the diffusion coefficient D_σ deduced from the Nernst–Einstein identity

$$D_\sigma = \frac{\sigma k_B T}{ne^2} \tag{36}$$

where n is the total concentration of alkali cations by unit volume and e is the elementary charge.

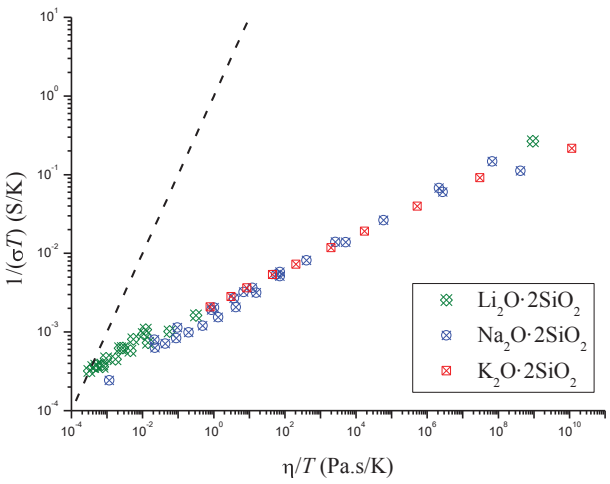

Figure 3. log(1/σT) versus log(η/T) in a log–log plot for lithium, sodium and potassium disilicates. The dashed line corresponds to an exponent of m=1 in Equation (38). Conductivity data were taken from several references cited in Ref. 4

If ionic transport and viscosity imply the same atomic transport mechanisms, $D_\eta=D_\sigma=D$, and a simple relation should link electrical conductivity and viscosity

$$\sigma T \propto D \propto \frac{T}{\eta} \tag{37}$$

This relation suggests a slope of 1 between $1/\sigma T$ and η/T in a log–log plot. Figure 2 shows such a representation for lithium, sodium and potassium disilicates. The three compositions in Figure 2 indicate a relation with good linearity but with a slope far from unity. This ionic transport-viscosity relation can thus be described by a so-called "fractional Stokes–Einstein"[68,69] equation

$$\sigma T \propto \left(\frac{T}{\eta}\right)^m \tag{38}$$

This fractional exponent depends on the ratio between the apparent activation energy involved in viscous flow and that for ionic transport at a given temperature. For all three compositions, the exponent m in Equation (38) is far from unity ($m\approx0{\cdot}2$), which confirms a significant difference in the transport mechanisms associated with ionic conductivity and viscous flow, as expected.

These two mechanisms involving different movements of chain segments leads to different relaxation processes, which might be identified as the α and β relaxations defined by Johari & Goldstein.[70] It is proposed that α relaxation is associated with long distance rearrangements with higher potential barriers, while β relaxation is restricted to more localized movements,[71,72] comparable to the SiO_4 tetrahedron vibrations. β relaxation remains an activated process

below the glass transition temperature. We suggest here that the activation energy involved in β relaxation, below T_g, might contribute to the activation energy for ionic conduction.

5. Conclusions

Experimental viscosity data of alkali disilicates were fitted by a DML equation containing two exponential terms, one of which is an Arrhenius type term while the other corresponds to a VFTH-like exponent. Introducing the free volume ratio ($V_\eta^{f*}/V_{0\eta}$) into the VFTH exponential, we obtained an expression with four variables: a pre-exponential term (A_η), an activation energy related to the Arrhenius term (E_η^A), the free volume ratio ($V_\eta^{f*}/V_{0\eta}$), and T_0 related to the VFTH term. Fixing A_η and T_0 at physically justifiable values, we obtained, by fitting, the two remaining terms, i.e. the Arrhenius activation energy and the $V_\eta^{f*}/V_{0\eta}$ ratio.

For the three alkali disilicates, the Arrhenius activation energy E_η^A was found to be 1·2 eV and the $V_\eta^{f*}/V_{0\eta}$ ratio close to 0·3. To discuss these results, we took into account previously determined activation energy (E_σ^A) and free volume ratio ($V_\sigma^{f*}/V_{0\sigma}$) related to ionic transport above the glass transition temperature. These data were obtained by fitting experimental ionic conductivity data on the three alkali disilicates under study with a similar DML equation as the one employed here for viscosity. For the ionic transport, the Arrhenius activation energy was found to be close to 0·5 eV and the free volume ratio close to 0·03. These results suggest that either the viscous flow or the ionic transport involves two different steps, an activated one described by the Arrhenius exponent and a second one that follows a VFTH expression.

We propose that, in the case of viscous flow, the activation energy E_η^A is related to the reorganization of covalent bonds involving bridging and nonbridging oxygen in the silicon tetrahedrons. A lower activation energy E_σ^A (0·5 eV) found for ionic transport is consistent with the proposed model, which predicts that this activation energy is associated to the formation of ionic pairs, and therefore involves weaker ionic bonds.

It was also found that both free volume ratios related to viscous flow ($V_\eta^{f*}/V_{0\eta}$) and to ionic transport ($V_\sigma^{f*}/V_{0\sigma}$) are relatively low, with the second one lower than the first. These results are in agreement with the idea that both viscous flow and ionic transport above T_g are assisted by low amplitude but different chain segment displacements. These displacements are probably limited to rotational and translational movements of SiO_4 tetrahedra in the case of viscous flow and to vibrations of nonbridging oxygens in the case of ionic transport. In the latter case, these vibrational movements would enable the transfer of the cationic pair from one nonbridging oxygen to another.

6. Acknowledgements

This work was financially supported by the Brazilian research funding agencies FAPESP (Process Nos. 2004/10703-0, 2007/08179-9, 2007/03563-5 and 2010/08003-0) and CNPq (305373/2009-9 and 479799/2010-5). JLS thanks the Vitreous Materials Laboratory (LaMaV-UFSCar) for its hospitality during his contribution to this paper.

7. References

1. Gutzow, I. & Schmelzer, J. W. P. *The Vitreous State*, Springer-Verlag, Berlin Heidelberg, 1995.
2. Kivelson, D., Tarjus, G., Zhao, X. & Kivelson, S. A. *Phys. Rev. E*, 1996, **53** (1), 751.
3. Sciglass 6.5, *SciGlass Dictionary* 2000–2004, Scivision.
4. Souquet, J. L., Rodrigues, A. C. M. & Nascimento, M. L. F. *J. Chem. Phys*., 2010, **132**, 034704.
5. Vogel, H. *Phys. Z*., 1921, **22**, 645.
6. Fulcher, G. S. *J. Am. Ceram. Soc*., 1925, **8**, 339.
7. Tamman, G. & Hesse, W. *Z. Anorg Allg. Chem*., 1926, **156**, 245.
8. Cohen, M. H. & Turnbull, D. *J. Chem. Phys*., 1959, **31**, 1164.
9. Adam G. & Gibbs, J. H. *J. Chem. Phys*., 1965, **43**, 139.
10. Dienes, G. J. *J. Appl. Phys*., 1953, **24**, 779.
11. Macedo, P. B. & Litovitz, T. A. *J. Chem. Phys*., 1965, **42**, 245.
12. Egelstaff, P. A. *An Introduction to the Liquid State*, Academic Press, London & New York, 1967.
13. Kumar, S. *Phys. Chem. Glasses*, 1963, **4** (3), 106.
14. Kauzmann, W. *Chem. Rev*., 1948, **43**, 219.
15. Richet, P. *J. Non-Cryst Solids*, 2009, **355**, 628.
16. Angell, C. A. & Sichina, W. *Ann. N.Y. Acad. Sci*., 1976, **53**, 279.
17. Angell, C. A. *J. Res. Natl. Inst. Stand. Technol*., 1997, **102**, 171.
18. Tanaka, H. *Phys. Rev. Lett*., 2003, **90** (5), 055701.
19. Mauro, J. C., Yue, Y., Ellison, A. J., Gupta, P. K. & Allana, D. C. *PNAS*, 2009, **106** (47), 19780.
20. Nascimento, M. L. F. & Aparicio, C. *Physica B*, 2007, **398**, 71.
21. Nemilov, S.V. *Thermodynamic and Kinetics Aspects of the Vitreous State*, CRC, Boca Raton, 1995.
22. Angell, C. A. *Pure Appl. Chem*., 1991, **63**, 1387.
23. Avramov, I. *J. Non-Cryst. Solids*, 2005, **351**, 3163.
24. Pfeiffer, T. *Solid State Ionics*, 1998, **105**, 277.
25. Bockris, J. O' M., Mackenzie, J. D. & Kitchener, J. A. *Trans. Faraday Soc*., 1955, **51**, 1734.
26. El-Badry, K., Ghoneim, N. A., El-Batal, H. A., Ammar, M. M. & Gharib, S. *Sprechsaal*, 1981, **114**, 599.
27. Fokin, V. M., Kalinina, A. M. & Filipovich, V. N. *J. Cryst. Growth*, 1981, **52**, 115.
28. Gonzalez-Oliver, C. J. R. PhD Thesis, University of Sheffield, 1979.
29. Heslin, M. R. & Shelby, J. E. *Boll. Soc. Espan. Ceram. Vidrio - Proc. XVI Intern. Congr. on Glass*, Madrid, 1992, **31-C**, 95.
30. Marcheschi, B. A. MsC Thesis, Alfred University, NY, 1985.
31. Ota, R., Tsuchiya, F., Kawamura, K., Nakanishi, S. & Fukunaga, J. *J. Ceram. Soc. Jpn*, 1991, **99**, 168.
32. Shartsis, L., Spinner, S. & Capps, W. *J. Am. Ceram. Soc*. **35**, 155 (1952).
33. Vasiliev, A. I. & Lisenenkov, A. A. In: *Proizvodstvo i Issledovanie Stekla i Silikatnykh Materialov*, 1978, Yaroslavl **6**, 144.
34. Wright, B. M. & Shelby, J. E. *Phys. Chem. Glasses*, 2000, **41**, 192.
35. Zanotto, E. D. PhD Thesis, University of Sheffield, 1982.
36. Zhenhua, Zeng *J. Chin. Silic. Soc*., 1986, **14**, 347.
37. Coenen, M. *Kolloid Z. Z. Polymere*, 1964, **194**, 136.
38. Ehrt, D., Leister, M., Matthai, A., Rüssel, C. & Breitbarth, F. *Proc. Fourth Int. Conf. Fundamentals of Glass Science and Technology*, Sweden, 1997, p204.
39. Fontana, E. H. & Plummer, W. A. *J. Am. Ceram. Soc*., 1979, **62**, 367.
40. Grussaute, H., Montagne, L., Palavit, G. & Bernard, J.-L. *Glastech. Ber. Glass Sci. Technol*., 2000, **73**, 380.
41. Hunold, K. & Bruckner, R. *Glastech. Ber*., 1980, **53**, 149.
42. Komleva, G. P. *Neorg. Mater*., 1971, **7**, 1285.
43. LaCourse, W. C. & Stevens, H. J. In: *Materials Science Research* **12**, *Borate Glasses*, Eds. L. D. Pye, V. D. Frechette & N. J. Kreidl, Plenum Press, NY, 1978, p539.
44. Leontjeva, A. A. *Zh. Fiz .Khim*., 1941, **15**, 134.
45. Lillie, H. R. *J. Am. Ceram. Soc*., 1939, **22**, 367.
46. Meiling, G. S. & Uhlmann, D. R. *Phys. Chem. Glasses*, 1967, **8**, 62.

47. Ota, R., Wakasugi, T., Kawamura, W., Tuchiya, B. & Fukunaga, J. *J. Non-Cryst. Solids*, 1995, **188**, 136.
48. Preston, E. *J. Soc. Glass Technol*., 1938, **22**, 45.
49. Scarfe, C. M., Mysen, B. O. & Virgo, D. *Carnegie Inst. Washington*, *Year Book*, 1979, **78**, 547.
50. Schnaus, U. E., Schroeder, J. & Haus, J. W. *Phys. Lett. A*, 1976, **57**, 92.
51. Shiraishi, Y., Nagasaki, S. & Yamashiro, M. *J. Non-Cryst. Solids*, 2001, **282**, 86.
52. Shvaiko-Shvaikovskaya, T. P., Mazurin, O. V. & Bashun, Z. S. *Neorg. Mater*., 1971, **7**, 143.
53. Skornyakov, M. M. In: *Fiziko-Khimicheskie Svoistva Troinoi Sistemy* Na_2O-PbO-SiO_2, Moskva, 1949, p39.
54. Sumita, S., Mimori, T., Morinaga, K. & Yanagase, T. *J. Jpn. Inst. Metals*, 1980, **44**, 94.
55. Suzuki, S., Kobayashi, T., Takahashi, M. & Imaoka, M. *Ann. Rep. Ceram. Eng. Res. Lab., Nagoya Inst. Technol*., 1980, **7**, 15.
56. Suzuki, S., Kobayashi, T., Takahashi, M. & Imaoka, M. *J. Ceram. Soc. Jpn*., 1981, **89**, 252.
57. Vasiliev, A. I., Lisenenkov, A. A. & Rashin, G. A. In: *Tezisy IV Simp. po Elektricheskim Svoistvam i Stroeniyu Stekla*, Erevan, 1977, p32.
58. Winter-Klein, A. In: *Stekloobraznoe Sostoyanie*, Moskva-Leningrad, 1965, p45.
59. Eipeltauer, E. & More, A. *Radex-Rundsch*., 1960, **4**, 230.
60. Farnan, I. & Stebbins, J. F. *Science*, 1994, **265**, 1206.
61. Doremus, R. H. *J. Appl. Phys*., 2002, **92** (12), 7619.
62. Klyuev, V. P. & Pevzner, B. Z. *Phys. Chem. Glasses*, 2004, **45**, 146.
63. Mazurin, O. V., Streltsina, M. V. & Shvaiko-Shvaikovskaya, T. P. (Editors), *Handbook of Glass Data, Physical Sciences Data No.1,5* Elsevier, Amsterdam, Vol. A, 1983, 249–250.
64. Charles, R. G. *J. Appl. Phys*., 1961, **32**, 1115.
65. Haven, Y. Verkerk, B. *Phys. Chem. Glasses*, 1965, **6** (2), 38.
66. Ingram, M. D., Mackenzie, M. A. & Lesikar, A. V. *J. Non-Cryst.Solids*, 1980, **38–39**, 371.
65. von Grotthus, C. J. D. *Ann.Chim*., 1806, **LVIII**, 54.
68. Voronel, A., Veliyulin, E., Machavariani, V. Sh., Kisliuk, A. & Quitmann, D. *Phys. Rev. Lett*., 1998, **80**, 2630.
69. Grandjean, A., Malki, M., Simonnet, C., Manara, D. & Penelon, B. *Phys. Rev. B*, 2007, **75**, 054112.
70. Johari, G. P. & Goldstein, M. *J. Chem. Phys*., 1970, **53**, 2372.
71. Prevosto, D., Capaccioli, S., Luchesi, M., Rolla, P. A. & Ngai, K. L. *J. Non-Cryst. Solids*, 2009, **355**, 705.
72. Nemilov, S. V. *J. Non-Cryst. Solids*, 2011, **357**, 1243.